SECOND EUROPEAN CONFERENCE ON EARTHQUAKE ENGINEERING
AND SEISMOLOGY, ISTANBUL AUG. 25-29, 2014

MAPPING GLOBAL EXPOSURE FROM SPACE: A REVIEW OF EXISTING PRODUCTS AND COMPARISON OF TWO NEW LAYERS OF GLOBAL URBAN EXTENT

Martin KLOTZ[1], Thomas KEMPER[2], Thomas ESCH[3], Martino PESARESI[4], Massimiliano PITTORE[5], Marc WIELAND[6], Christian GEISS[7] and Hannes TAUBENBÖCK[8]

ABSTRACT

In order to assess and quantify earthquake risk over large spatial extents on a global or regional scale spatial data localizing human assets is on strong demand. However, due to the large-scale extent of human activities on our planet, the scientific community has been lacking tools and methodologies to capture the entity of elements at risk, especially with enhanced thematic and geometric detail on global scale. First generation of global land cover datasets and maps of urban extent produced since the millenium relied on coarse resolution satellite sensors such as MODIS or DMSP-OLS. Despite the availability of finer scale imagery no other product of global coverage has been made available until today. However, global human exposure mapping from remote sensing is now entering a new era and new products currently in the making such as the Global Urban Footprint and the Global Human Settlement Layer will deliver spatial information on human settlements at unprecedented spatial resolutions. Once available on a global scale, these layers will improve significantly the knowledge base for the localization of human assets with regard to georisks. This work reviews past mapping products of coarse geometric resolution and further presents first validation efforts of the two new layers based on standard accuracy measures with regard to a geometrically and thematically highly resolved building reference. This first assessment reveals that the high resolution settlement layers produce comparable outputs that are capable of mapping even smaller settlements in low-density rural areas although significant over-classification due to the specific characteristics of each classifier is obvious. To gain a deeper understanding of these layers further validations efforts using pattern-based regression analysis and measures of inter-map agreement are currently underway.

INTRODUCTION

A definition that is exhaustively used for the term exposure in the earthquake risk community describes elements at risk, which are understood as objects potentially adversely affected such as people, properties, infrastructure or economic activities (Geiß & Taubenböck, 2012). Thus, the determination of potential losses from damaging events within the context of state-of-the-art seismic

[1] MSc, German Aerospace Center (DLR), Weßling, martin.klotz@dlr.de
[2] Dr, Joint Research Center (JRC), Ispra, thomas.kemper@ec.jrc.europa.eu
[3] Dr, German Aerospace Center (DLR), Weßling, thomas.esch@dlr.de
[4] Dr, Joint Research Center (JRC), Ispra, martino.pesaresi@ec.jrc.europa.eu
[5] Dr, German Research Center for Geoscience (GFZ), Potsdam, marc.wieland@gfz-potsdam.de
[6] Dr, German Research Center for Geoscience (GFZ), Potsdam, massimiliano.pittore@gfz-potsdam.de
[7] MSc, German Aerospace Center (DLR), Weßling, christian.geiss@dlr.de
[8] Dr, German Aerospace Center (DLR), Weßling, hannes.taubenboeck@dlr.de

risk models such as HAZUS (FEMA, 2010), OpenQuake (GEM, 2011) or RiskScape (RiskScape, 2012) is supported by combining hazard parameters but also quantified and characterized exposed elements and their assessed vulnerability. Despite the fuzzy definition of the term exposure, it is clear that it is of crucial importance for a comprehensive understanding of risk and presents an essential component for a comprehensive vulnerability assessment.
Remote sensing for vulnerability-centred investigations is a less long established field of research compared to hazard analysis and most of the past studies either only deal with the overall evaluation of the capabilities of remote sensing (e.g. Taubenböck et al., 2008) or explicitly address individual vulnerability components (e.g. Mueller et al., 2006). However, in recent years, valuable research has been carried out contributing to different vulnerability aspects of geo-risks by the employment of remote sensing-based methods, concepts and data, especially focusing on the capturing, delineation and characterization of elements at risk in urban landscapes across various spatial scales.

On the local scale, the potential of remote sensing particularly lies in the generation of spatially accurate building inventories for the detailed analysis of the building stock's physical vulnerability (French & Muthukumar, 2006; Mueller et al., 2006; Taubenböck et al., 2009; Polli & Dell'Acqua, 2011). For urban areas, mapping efforts specifically relate to the capturing of elements at risk of the built environment such as buildings and infrastructures. Vulnerability-related indicators have been derived in various earthquake-related studies and include building footprint, height, shape characteristics, roof materials, location, construction age and structure type (Geiß & Taubenböck, 2012). Especially last generation optical sensors featuring very high geometric resolutions are perceived as advantageous for operational applications, especially for small to medium scale urban areas (Deichmann et al., 2011). These data are found to be suitable to quantify and characterize the building stock based on manual image analysis methods, statistical enumeration of samples (Ehrlich et al. 2010) or automatic image information extraction methods (Sahar et al. 2010; Borzi et al. 2011). By the combination of optical sensors with digital elevation information from LIDAR seismic buildings vulnerability can be determined with high accuracies (Borfecchia et al., 2010) whereas the combination of optical and SAR data has proven useful for the retrieval of crucial physical parameters such as building footprint or height (Polli & Dell'Acqua, 2011). Beyond, medium to high resolution remote sensing data is suited to characterize homogeneous built-up areas. In this manner, Pittore and Wieland (2012) and Wieland et al. (2012) use this capability in combination with information from a ground-based omnidirectional imaging system to determine the physical vulnerability of the building inventory.

Although local mapping efforts employing high resolution satellite data can be used to directly derive structural characteristics of buildings and their performance under earthquake stress, they lack the capabilities to capture the entity of elements at risk for large-scale urban areas as an essential input for a global to regional risk analysis and rapid loss estimation. On the regional and global scale, remote sensing derived geo-products are well suited to approximate the inventory of elements at risk in their spatial extent and abundance by mapping and modelling approaches of land cover or related spatial attributes such as night-time illumination (e.g., Elvidge et al., 2009) or fractions of impervious surfaces (e.g., Elvidge et al, 2007). Furthermore, these spatial information are commonly used as a basis for the disaggregation of demographic or socioeconomic variables (Eicher & Brewer, 2001; Mennis & Hultgren, 20006; Langford, 2007) and present a first localization of exposed assets in the context of sampling approaches. From this, it becomes clear that global datasets present a valuable basis for the analysis of large-scale human exposures and a first approximation of their spatial distribution. On the global scale several efforts have been undertaken since the millennium to provide land cover / use maps with a particular focus on mapping urban areas and spatial representations of physical variables related to human exposure. These large-scale global products are especially important as they present the almost only data source for systematic risk analysis in data-poor countries. In this regard, various geospatial information layers and approaches to model and assess situation-specific physical and human exposure are presented by Aubrecht et al. (2012) and validated by Pottere and Schneider (2009) as well as Pottere et al. (2009).

This paper presents a review of past mapping efforts and products related to global exposure conducted in the context of EU FP7 Project SENSUM (Framework to integrate Space-based and in-situ sENSing for dynamic vUlnerability and recovery Monitoring). For the review and exemplification of global exposure data a multi-source and multi-scale exposure database has been set-up to showcase the technical capabilities of the respective information layers including multi-category land cover datasets, global layers of urban extent and map representations of spatially continuous variables related to human exposure. The database covers the spatial extent of the city of Cologne, Germany. Information is given on the technical specifications of these products, the methodologies and input data employed for generation and previous validation efforts. In the following, first validation results from the accuracy assessment of two new layers of global urban extent, namely DLR's Global Urban Footprint (GUF, Esch et al. 2013) and JRC's Global Human Settlement Layer (GHSL, Pesaresi et al., 2013) with regard to a large-scale and highly resolved building reference layer are presented.

REVIEW OF GLOBAL EXPOSURE DATASETS

Accurate and up-to-date global land cover data sets can provide a valuable first level approximation of human developed land prone to or affected by a possible natural hazards. In recent years, substantial advancement has been achieved in generating such *multi-category land cover products* on the global scale:

The Global Land Cover 2000 (GLC) has been initiated by the European Commission's Joint Research Center (JRC) (JRC, 2003). The database contains a detailed, regionally optimized land cover data base for each continent and a less thematically detailed global legend. The datasets are mainly derived from daily data from the VEGETATION sensor on-board SPOT-4. The land cover inventory covers a range of 22 thematic classes including one for artificial surfaces and associated areas at a geometric resolution of 30 arcseconds (ca. 1km). The map was derived applying a "regionally tuned" supervised classification method on combinations of multispectral and multi-temporal EO data (Bartholome & Belward, 2005). Due to its long-time existence the GLC product has been thoroughly tested in previous validation efforts. Mayoux et al. (2006) analyzed the classification accuracy using ground observations, previously generated land cover maps and high-resolution satellite imagery for stratified random sampling of reference datasets stating a global overall accuracy of 68.8 percent.

GlobCover is a global land cover product that has been first published in 2005 and updated in 2009 under the lead of the European Space Agency (ESA). With a spatial resolution of ca. 300m it provided the very first medium resolution global land cover in 2005 (ESA, 2010). Like GLC it features 22 thematic land cover classes, one dedicated to artificial surfaces and associated areas defined as pixels having an urban area percentage of greater than 50 percent. GlobCover employs automated land cover classification by a sequential execution of regional stratification, spectral clustering, and rule-based class labelling using data from the Medium Resolution Imaging Spectrometer (MERIS) on-board ENVISAT. ESA (2011) has validated the GlobCover product by setting up a reference dataset of random points collected from various external information sources (e.g. Google Earth, Virtual Earth, Open StreetMap, SPOT-4 VEGETATION, etc.) and state an overall thematic accuracy of 70.7 percent. Potere & Schneider (2009) determine even higher overall accuracies exceeding 96 percent for urban areas and a strong agreement with the GLC dataset by inter-map comparison.

The MODIS Land Cover Type by the United States Geological Survey (USGS, 2013) is updated annually and contains five classification schemes based on data of the Moderate Resolution Imaging Spectrometer (MODIS) on-board the National Aeronautics and Space Administration's (NOAA)Terra and Aqua satellites. Its primary legend established in the context of the International Geosphere Biosphere Programme (IGBP) identifies 17 land cover classes, one dedicated to urban and built-up areas. The data is provided at a geometric resolution of 15 arcseconds (ca. 500m) and has been derived based on a supervised decision-tree classification method using multispectral and thermal input data as well as ancillary such as Landsat or Geocover 2000 imagery for training and classification refinement.

Results from a cross-validation conducted by Friedl et al. (2010) indicate an overall thematic accuracy of 75 percent with a relatively wide range of class-specific accuracies.

Table 1 Overview of global multi-category landcover datasets

	Global Land Cover	***Globcover***	***MODIS Land Cover***
Quicklook	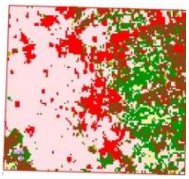	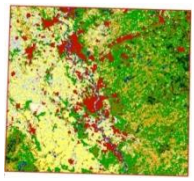	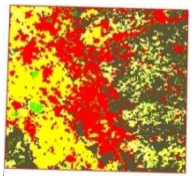
Spatial resolution	1,000m	300m	500m
Thematic resolution	22 thematic classes (1 urban)	22 thematic classes (1 urban)	17 thematic classes (1 urban)
Year	2000	2005 / 2009	2012
Originator	JRC	ESA	USGS

On the regional and global scale, remote sensing can further be employed to map *spatially continuous variables related to human exposure* and thus, approximate the inventory of elements at risk in their spatial extent and abundance. Spatial attributes commonly related to human activities are for example night-time illumination and the degree of soil sealing or artificial surfaces (Table 2):

The Global Impervious Surface Area (IMPSA) presents the global distribution and density of impervious surfaces at a spatial resolution of 30 arcseconds (ca. 1km) (Elvidge et al., 2007). For product generation, it mainly uses coarse resolution input data such as the DMSP-OLS Nighttime Lights time series from the reference years 2000 and 2001 as well as the LandScan 2004 gridded population database. Schneider and Potere (2009) thresholded IMPSA to determine urban extents and derived an absolute accuracy measures of 97.5% inlcuding low errors of commission and omission. In addition to that Elvidge et al. (2007) found a significant correlation between reference data of the United States and IMPSA, however, state a moderate over-classification in states of small but highly urbanized areas (urban hotpsots).

The Operation Linescan Sensor (OLS) oboard the Defense Meteorological Satellite Program's (DMSP) satellites records time series monitoring the intensity of stable lights of the earth's surface and thus provides useful for measuring stable human settlements and spatiotemporal urbanization through this indicator (Elvidge et al., 2009). Since 1992, several nighttime light products have been derived, one of them being a global cloud-free coverage especially designed to detect changes of human emitted lighting and thus, spatiotemporal urbanization processes. Although featuring a coarse resolution of roughly 1 km the dataset has been widely employed in modelling the spatial distribution of population or human activity and has been used as input to many other global land cover products (Potere et al., 2009).

LandScan is a commercial global population distribution dataset providing information in gridded format produced by the Oak Ridge National Laboratory (ORNL). It is today the highest resolution global population global database regarding spatial population distribution (ORNL, 2013) and data has been widely applied for modelling the spatial distribution of human assets at risk (Dobson et al., 2000). At 30 arcseconds (ca. 1 km) LandScan maps the ambient population averaged over 24 hours. It uses high resolution EO imagery from sensors such as SPOT as well as various additional data sources such as EO derived land cover products, roads and populated places, digital terrain models (DTM), nighttime lights as well as national and subnational population statistics for disaggregation through a multivariate dasymetric modelling approach. To verify and validate the modelling approach Dobson et al. (2000) quantified the correspondence with highest resolution census counts for the South western United States (87.8 percent) and Israel (91 percent).

Table 2 Overview of global maps representing spatially continuous variables related to human exposure

	Global Impervious Surface Area	***DMSP-OLS Nighttime Lights***	***Landscan***
Quicklook	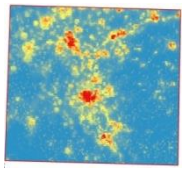	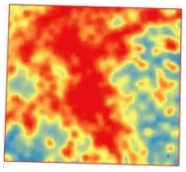	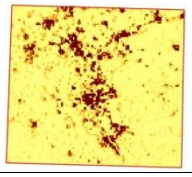
Spatial resolution	*1.000m*	*1.000m*	*1.000m*
Thematic resolution	*Impervious Surface fraction (%)*	*Intensity of stable lights (DN x percent frequency)*	*Ambient human pupulation (count per gridcell - 24h avg.)*
Year	*2000/2001*	*1992-2013*	*2010-2012*
Originator	*NOAA*	*NOAA*	*ORNL*

Although a clear and univocal delineation of urban areas is not trivial at a global scale due to significant variations of thematic definitions associated with this term (Taubenböck et al., 2012), the goal of many global urban mapping efforts is the generation of current, consistent and seamless maps of urban, built-up and settled areas for the Earth's land surface. In this regard, Potere and Schneider (2009) and Potere et al. (2009) give a thorough review of some of these *maps of global urban extent* listed in table 3.

The Global Rural-Urban Mapping Project's Urban Extent layer which was last updated in 1995 is a low resolution map elaborated by the Columbia University's Socioeconomic Data and Applications Center (SEDAC) representing binary information on the existence of global / rural extents (SEDAC, 2013). The product was derived using NOAA's DMSP-OLS nighttime light product from the reference period1994 to 1995 to detect stable human settlements. Furthermore, ancillary data was provided by the Digital Chart of the World's (DCW) populated places inventory for initial localization of human settlements at a scale of 1:1,000,000 (SEDAC, 2013). In addition to that, for areas of inadequate or limited electrical power sources the urban extents were extrapolated using a population-area ratio. In their investigations, Potere and Schneider (2009) as well as Potere et al. (2009) compared GRUMP to Landsat derived reference maps of urban extent from 140 cities around the globe and found overall accuracies of 84 percent – the lowest for all datasets assessed – featuring very high errors of commission and low inter-map agreement to other global products.

The global MODIS Urban Land Cover map was produced at the Center for Sustainability and the Global Environment (SAGE) at the University of Wisconsin-Madison (Schneider et al, 2009 & 2010). The higher-ranking goal of this project was to produce a seamless map of urban extent for the years 2001 and 2002. In this context urban, areas are defined as places that are dominated by the built environment which include a mix of human-made surfaces and materials greater or equal to 50 percent of a pixel. For spatial derivation multispectral MODIS data of 500m geometric resolution were employed through a sequential execution of region-specific stratification of eco-regions, decision tree classification based on training data from manual interpretation, and posteriori exploitation of class membership functions for classification optimization (Schneider et al., 2010).
Using the same reference maps as for GRUMP the dataset yields an overall per-pixel accuracy of 93 percent (*Kappa=0.65*) (Schneider et al., 2010).

In this context mapping global urban extent, the two currently developed global products promise to be a major leap forward regarding the derivation of high resolution and accurate reference data for human exposures on a global level. With the GUF and the GHSL both featuring a spatial resolution of ≤ 12m these layers will provide consistent, up-to-date and geometrically detailed land cover information on unprecedented spatial detail in the near future. However, both layers are still in the

phase of testing and refinement. Thus, validation efforts and analysis on the absolute accuracies are currently investigated by DLR to to gain a stronger understanding of each map's strength and weakness.

Table 3 Overview of new and existing global maps of urban extent

	Global Rural Urban Mapping Project	***MODIS Urban Land Cover***	***Global Human Settlement Layer***	***Global Urban Footprint (GUF)***
Quicklook		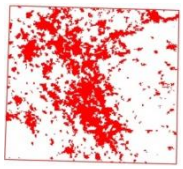	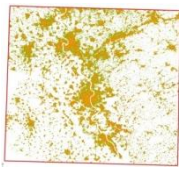	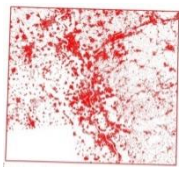
Spatial resolution	*1.000m*	*500m*	*0.5-10m*	*12m*
Thematic resolution	*Urban / Non-urban*	*Urban / Non-urban*	*Urban / Non-urban*	*Urban / Non-urban*
Year	*1995*	*2001/2002*	*2011-2013*	*2011/2012*
Originator	*SEDAC*	*SAGE*	*JRC*	*DLR*

STUDY SITE AND DATA

The accuracy assessment of the GUF and GHSL focuses on a square area of 100 by 100 km^2 covering diverse settlement patterns of urban and rural character in western Germany, including the city of Cologne, the metropolitan Ruhr area as well as the rural Sauerland region (Figure 1). The area of interest was further determined by the availability of optical imagery for GHSL generation as well as very high resolution synthetic aperture radar data for GUF production. Furthermore, for the determination of absolute accuracies, building footprints of more than 900,000 buildings were extracted as a reference layer from German topographical map (DTK 1:25,000).

The GUF classification is based on radar satellite data from the German space missions TerraSAR-X (TSX) and TanDEM-X (TDX) which have collected two coverages of the entire land-mass for 2011 and 2012. In this context, the German Aerospace Center (DLR) has developed a pixel-based classification approach aiming to globally extract urban and non-urban structures from the single-look radar imagery. The high resolution SAR imagery acquired in Stripmap mode used to map the GUF is processed by extracting texture information, which is suitable for highlighting regions characterized by highly structured and heterogeneous built-up areas. From these texture features binary settlement information (presence/absence of built-up areas) of an unprecedented geometric resolution of 12m is derived based on an unsupervised classification scheme accounting for both the original backscattering amplitude and the extracted textural information (Esch et al. 2013). Considering the challenges of global urban mapping, the algorithm is currently further investigated for the potential to improve the classification performance by substituting the presented threshold-based technique by a machine-learning approach (Esch et al., 2012).

JRC's classification of the Global Human Settlement Layer is based on high resolution SPOT data of 2.5m spatial resolution. The GHSL automatic image information extraction workflow integrates multi-resolution (0.5m-10m), multi-platform, multi-sensor (PAN, multispectral), and multi-temporal raw optical image data such as SPOT-4/5, Quickbird, Ikonos or airborne sensors (JRC, 2012) using a combination of textural and morphological algorithms that are combined with innovative learning approaches (Pesaresi et al., 2013). The extracted features are subsequently classified and spatially generalized into a binary information layer of built-up and non built-up areas.

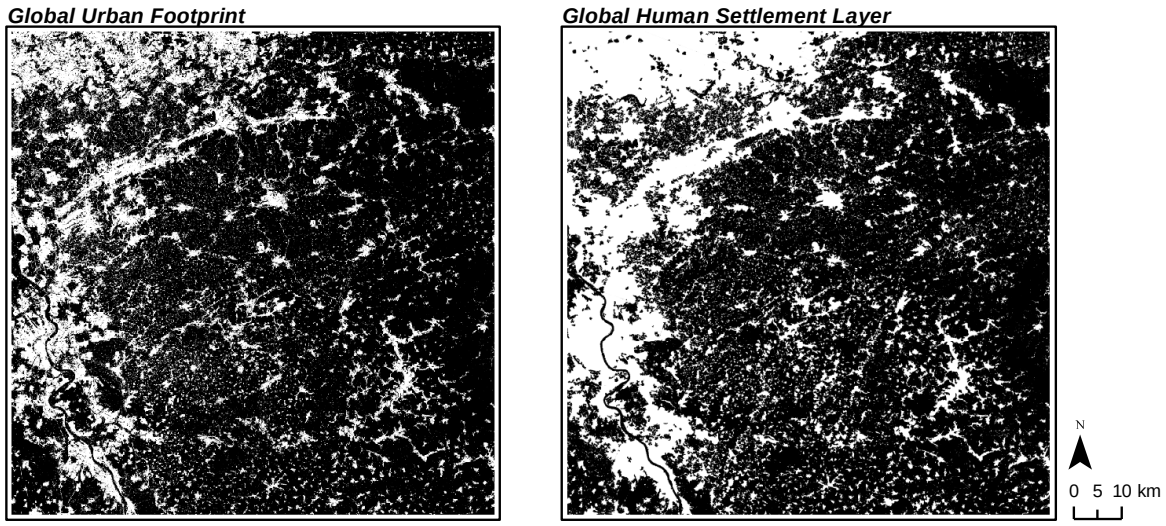

Figure 1 GUF and GHSL classifications derived for the 100km by 100km test site in Western Germany

METHODS

Assessing the accuracy of land cover data is one of the main challenges in the field of mapping urban areas. This is on the one hand due to the lack of spatially consistent, up-to-date and area-wide reference data (Taubenböck et al., 2011) and on the other hand related to the discussion on an adequate selection of meaningful agreement measures (McPherson et al, 2004; Allouche et al., 2006; Liu et al.; 2007; Taubenböck et al., 2011). Nevertheless, it is now widely recognized in today's scientific community that no classification is valid or complete until a certain degree of confidence of the mapping accuracy has been gained. Error or confusion matrices are an often used approach which mostly use randomly distributed test sites leading to a descriptive evaluation by standard measures of agreement between the validation data and the classification output (Taubenböck et al., 2011). These standard measures often include the producer's accuracy to determine the error of commission of allocated pixels as well as the user's accuracy as a measure of the omission. However, there is broad consensus in the scientific literature that metrics based on the entire error matrix add significant value to the accuracy assessment beyond these basic measures. A thorough review of the standard accuracy measures, problems encountered when using them and remarks on meaningful interpretation is given by Foody (2008).

As a first step to assess the capabilities of mapping of urban areas, both maps of global urban extent are visually and quantitatively compared to the reference dataset on object level to determine the share of buildings captured by these layers. From this, the error of omission regarding missed buildings is calculated. These basic descriptive measures establish a general degree of completeness of the classified settlement pattern as defined by building inventory, however, do not comprise information on its overall correctness and quality.

Table 4 Contingency table for a two-class map comparison (from Potere & Schneider, 2009)

		Validation data	
		Presence	Absence
Settlement layer	Presence	*a*	*b*
	Absence	*c*	*d*

For further comparison of the two layers of global urban extent a wider set of accuracy measures is calculated on a per-pixel basis as recommended by Foody (2008). These are based on two-class contingency tables resulting from the overlay of the settlement layers and the high resolution

validation data and record the number of true positives (a), false positives (b), true negatives (c) and false negatives (d) (Table 4). These allow for the calculation of several quantitative measures of agreement (Table 5):

- **Overall accuracy** measures the classification accuracy as the share of all correctly classified urban and non-urban pixels in the error matrix and thus, gives general information regarding the overall map accuracy. However, this measure does not take into account unequal class distributions and thus, does not paint a detailed picture of the accuracy across individual land cover classes.

- **Sensitivity (Completeness)** relates to the ability/probability to classify urban pixels as defined by the building reference correctly. It is the percentage of the building reference data which corresponds to the classification output of the respective urban extent layer and is closely related to the error of omission (1-sensitivity). The ideal value for the completeness is 100 percent. In turn, the ability of classifying the absence of urban areas correctly is called *specificity*.

- **Precision (Correctness)** relates to the classifier's ability to exclude non-urban areas correctly from the urban extent classification as defined by the building reference. This measure is closely related to the error of commission (1-precision) and reaches and ideal value of 100 percent.

- **Kappa statistic (K)** is designed to measure the strength of agreement between the reference data and the classification output, taking into account the potential for chance agreement. *K* considers all information in the error matrix and ranges on a scale of 0 to 1 where the latter indicates perfect agreement. Congalton (1991) categorizes Kappa into three groups of strong agreement (≥0.8), moderate agreement (0.4-0.8) and poor agreement (≤0.4).

- **True Skill Statistic (TSS)** is – like Kappa – designed to measure the agreement between the classification and the building reference layer. It is calculated as the specificity (fraction of correctly classified urban pixels) plus the sensitivity (fraction of correctly classified non-urban pixels) minus one. Compared to Kappa it has the advantage of being independent from unequal class distributions, i.e. prevalence (*(a+c)/n* which is the proportion of pixels assigned to buildings in the reference dataset), and thus provides a more robust measure of classification accuracy (Allouche et al., 2006). Its range spans from negative values (systematic disagreement) to 1 (perfect agreement), with a value of 0 indicating a random classification result.

Table 5 Map agreement measures used in this work; in all formulae n = a + b + c + d (Allouche et al., 2006)

Measure	Formula
Overall accuracy	$\frac{a+d}{n}$
Sensitivity (Completeness)	$\frac{a}{a+c}$
Precision (Correctness)	$\frac{a}{a+b}$
Kappa statistic (K)	$\frac{\left(\frac{a+d}{n}\right) - \frac{(a+b)(a+c)+(c+d)(d+b)}{n^2}}{1 - \frac{(a+b)(a+c)+(c+d)(d+b)}{n^2}}$
True Skill statistic (TSS)	$sensitivity + specificity - 1$

RESULTS

A first visual comparison of the GUF and GHSL products reveals that the new layers hold great potential for mapping the spatial outline of settlement patterns in a very detailed manner. Beyond the localization of high density urban areas of large cities, both layers seem to detect also smaller settlement patches featured by low building numbers scattered in the rural landscape (Fig. 2). Both layers detect a similar share of the building inventory on object level: While the GUF captures 87.6 percent of the entire building stock, the GHSL reaches a share of even 92.3 percent. From this, the error of omitted buildings amounts to 12.4 percent for the GUF and 7.7 percent for the GHSL. These basic descriptive measures establish a first impression regarding the degree of completeness of the classified settlement pattern as defined by building inventory.

More robust and detailed information on the overall accuracy of the classification results can be drawn from the extended set of accuracy measures calculated from the error matrices of the respective layers (Tab. 6). For both datasets, the results indicate good overall classification accuracies of 84.8 and 73.4 percent, respectively. This constitutes a high robustness of the classification process, leading to the preliminary assumption that both classifiers – when applied to an arbitrary city of diverse urban pattern - generally produce a correct delineation of urban from non-urban pixels as defined by the spatial arrangement of the building inventory.

The analysis of completeness und correctness allows for a more detailed, class-specific insight into the accuracy of the urban maps. In line with the analysis on object level, high sensitivity of both GHSL (97.6 percent) and GUF (90.1 percent) underline the capabilities of capturing the entity of built-up objects, painting an almost complete picture of the urban extent based on the outline of the building pattern. This is further manifested by high specificity values for the absence of urban pixels. In contrast, the low precision values presented relate to classification of a high share of pixels not belonging to the building mask and thus, expose significant errors of commission in both layers. Low correctness induced by over-classification of urban areas in both classifiers is also reflected in the poor agreement represented by the Kappa scores for the GUF (0.32) and the GHSL (0.20). On the one hand, this is due to the fact that a high-detailed building reference is used for validation which goes beyond the geometric capabilities of the datasets under study by clearly delineating buildings from intra-urban spaces. In contrast, both GUF and GHSL rather aim to map the outline of the settlement pattern as defined by the reference data. At this point, a viable option would be the integration of further elements of the urban landscape like roads, bridges, urban greenery, etc. into the reference to obtain a more realistic picture of the settlement pattern. Thus, this result reveals that both layers in their current configuration do not map a building layer, but map the pattern of the urban extent. On the other hand, the limited spatial precision and capabilities to map individual buildings can be attributed to the particular technical specifications of each classifiers information extraction workflow: While GUF processor extracts urban and non-urban areas from single-look radar imagery based on texture information characteristic for highly structured and heterogeneous built-up areas by e.g. double-bounce detection and high-intensity backscattering (Esch et al., 2010) the GHSL applies a spatial generalization technique between detected built-up structures to account for the trade-off between precision and operational cost (Pesaresi et al., 2013).

Finally, TSS presents a more robust measure with regard to the unequal class distribution inherent in the reference data and thus, assesses the overall spatial delineation urban and non-urban areas with regard to the diverse landscape of urban and rural character. From the high values of 0.74 for the GUF and 0.69 for the GHSL it can be concluded that the new global products identify and delineate urban extent in its correct dimension and outline although not mapping the geometrically and thematically highly detailed reality as represented by the building inventory.

Table 6 Overview of the selected accuracy measures derived for the GUF and GHSL classifications on test site level with regard to the building reference

	GUF	GHSL
Overall Accuracy [%]	84.82	73.35
Sensitivity (Completeness) [%]	90.14	97.62
Specificity [%]	84.54	72.05
Precision (Correctness) [%]	23.76	15.74
Kappa statistic	0.32	0.20
True Skill statistic	0.74	0.69

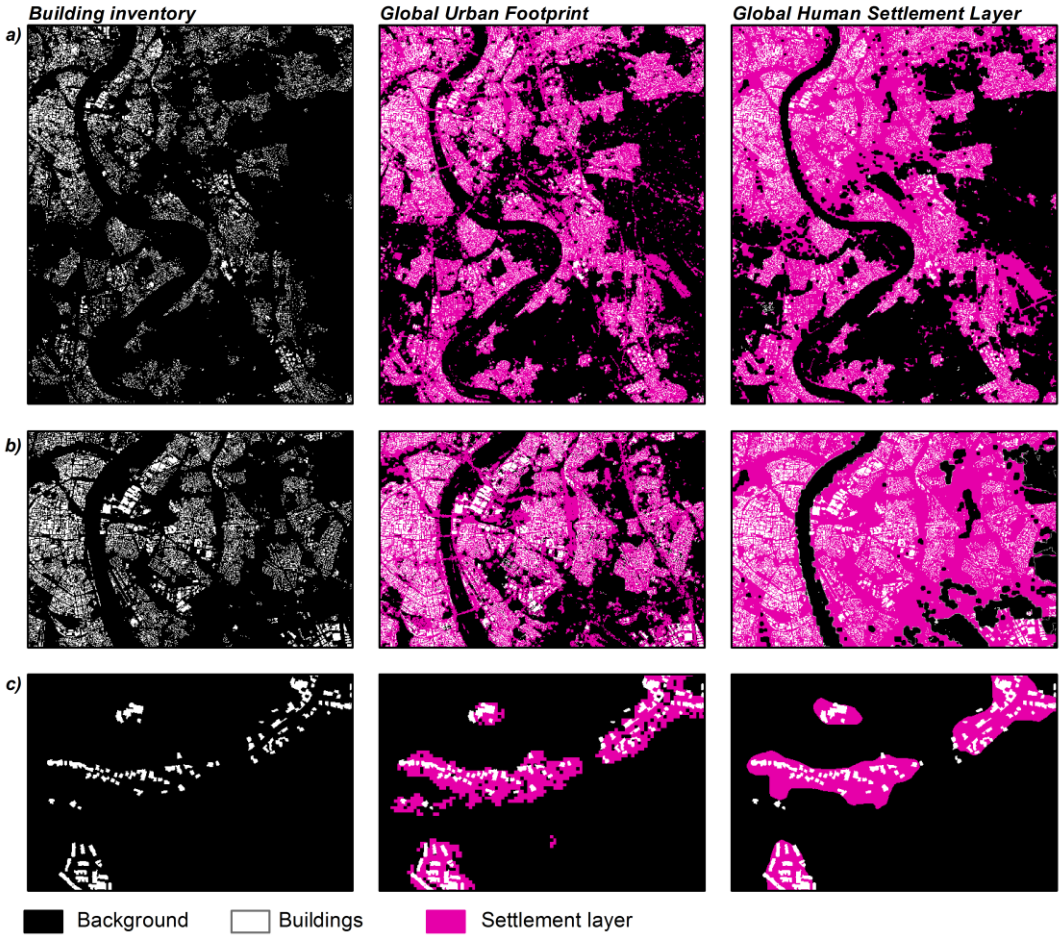

Figure 2 Visual comparison of the building reference layer, GUF and GHSL for (a) the city of Cologne and exemplified for b) high built-up density urban fabric and c) low density rural areas

From this initial accuracy assessment it becomes clear that both of the two new maps of global urban extent provide comparable outputs. While the GHSL performs slightly better in capturing the entity of objects of the spatial building pattern it also features higher errors of commission. Both layers further proof to be capable of spatially delineating the overall settlement pattern as outlined by the building inventory, however, feature limited capabilities in terms of per-building correctness and precision. Beyond this first assessment, further validation efforts using pattern-based regression analysis and measures of inter-map agreement are currently underway to gain a deeper understanding of the consistency of both layers, explore structural dependencies classification and determine pattern-based characteristics of each classifier.

CONCLUSION

The review of existing products capable of localizing human exposure on a global scale highlights the need for higher resolution data especially for large-scale urban landscapes of varying structural character. First generation global land cover datasets and map representation of spatially continuous variables related to human exposure have been mainly produced based on coarse resolution satellite sensors such as MODIS or DMSP-OLS in the range of 300m to 1,000m. In contrast, the GUF and the GHSL present current mapping efforts employing finer scale optical and radar imagery which will provide information on global urban extent at an unprecedented geometric resolution and detail.

An initial accuracy assessment based on standard measures of agreement derived from the overlay of the respective layers and a high resolution building reference reveals comparable results. Both products are capable of correctly and completely outlining the settlement pattern as defined by the building inventory, mapping even smaller settlements in low-density rural areas. Nevertheless, significant over-classification due to the specifications of each particular information extraction workflow exists leading to the clear understanding that the new layers do not present high resolution building masks but rather spatially highly detailed settlement layers.

ACKNOWLEDGEMENT

We want to acknowledge the support by the European Commission's Seventh Framework Programme [FP7/2007-2013], under grant agreement no. 312972 "Framework to integrate Space-based and in-situ sENSing for dynamic vUlnerability and recovery Monitoring".

REFERENCES

Allouche, O., Tsoar, A., Kadmon, R. (2006) Assessing the accuracy of species distribution models: prevalence, Kappa and true skill statistic (TSS). Journal of Applied Ecology, 43, 1223-1232.

Aubrecht, C., Özceylan, D., Steinnocher, K., Freire, S. (2012) Multi-level geospatial modeling of human exposure patterns and vulnerability indicators. In: Taubenböck, H., Post, J., Strunz, G. (eds.) Remote sensing contributing to mapping earthquake vulnerability and effects. Special Issue in Natural Hazards.

Bartholome, E., Belward, S. (2005) GLC2000: a new approach to global land cover mapping from Earth observation data. International Journal of Remote Sensing, 26, 2005.

Borfecchia, F., Pollino, M., De Cecco, L., Lugari, A., Martini, S., La Porta, L., Ristoratore, E., Pascale C (2010) Active and passive remote sensing for supporting the evaluation of the urban seismic vulnerability. Italian Journal of Remote Sensing, 42,129–141.

Borzi, B., Dell'Acqua, F., Faravelli, M., Gamba, P., Lisini, G., Onida, M., Polli, D. (2011) Vulnerability study on a large industrial area using satellite remotely sensed images. Bulletin of Earthquake Engineering, 9, 675–690.

Congalton, R.G. (1991) A review of assessing the accuracy of classification of remotely sensed data. Remote Sensing of Environment, 37, 35–46.

Deichmann, U., Ehrlich, D., Small, C., Zeug, G. (2011) Using high resolution satellite data for the identification of urban natural disaster risk. Global Facility for Disaster Reduction and Recovery, Washington, DC.

Dobson, J. E., E. A. Bright, P. R. Coleman, R. C. Durfee, B. A. Worley. 2000. "A Global Population database for Estimating Populations at Risk", Photogrammetric Engineering & Remote Sensing Vol. 66, No. 7, July, 2000.

Ehrlich, D., Zeug. G., Gallego, J., Gerhardinger, A., Caravaggi, I., Pesaresi, M. (2010) Quantifying the building stock from optical high-resolution satellite imagery for assessing disaster risk. Geocarto International, 25(4), 281–293.

Eicher, C.L., Brewer, C.A. (2001) Dasymetric mapping and areal interpretation interpolation: implementation and evaluation. Cartography and Geographic Information Science, 28, 125-138.

Elvidge, C., Tuttle, B.T., Sutton, P.C., Baugh, K.E., Howard, A.T., Milesi, C., Budhendra, B.L., Ramakrishna, N. (2007).Global distribution and density of constructed impervious surfaces. Sensors, 7,1962−1979.

Elvidge, C.D., Erwin, E.H., Baugh, K.E., Ziskin, D., Tuttle, B.T., Ghosh, T., Sutton, P.C. (2009) Overview of DMSP nighttime lights and future possibilities. In Proceedings of the 7th International Urban Remote Sensing Conference, Shanghai, China, 20–22 May 2009.

Esch, T., Marconcini, M., Felbier, A., Roth, A., Heldens, W., Huber, M., Schwinger, M., Müller, A. (2013): Urban Footprint Processor – Fully automated processing chain generating settlement masks from global data of the TanDEM-X mission. Geoscience and Remote Sensing Letters, Special Stream EORSA2012. Submitted.

Esch, T., Taubenböck, H., Roth, A., Heldens, W., Felbier, A., Thiel, M., Schmidt, M., Müller, M., Müller, A., Dech, S. (2012) TanDEM-X mission—new perspectives for the inventory and monitoring of global settlement patterns. Journal of Applied Remote Sensing, 6, 061702.

European Space Agency (2010) GlobCover 2009 Product Description Manual. Available at: http://dup.esrin.esa.it/files/p68/GLOBCOVER2009_Product_Description_Manual_1.0.pdf Accessed: 4 Oct 2013.

European Space Agency (2011) Product Description and Validation Report. Available: http://due.esrin.esa.int/globcover/LandCover2009/GLOBCOVER2009_Validation_Report_2.2.pdf Accessed 4 Oct 2013.

FEMA (2010) HAZUS—MH MR5. Multi-hazard loss estimation methodology—earthquake model. Technical manual. Department of Homeland Security, Emergency Preparedness and Response Directorate. Washington D.C.

Foody, G.M. (2008) Harshness in image classification accuracy assessment. International Journal of Remote Sensing, 29, 3137–3158.

French S.P., Muthukumar, S. (2006) Advanced technologies for earthquake risk inventories. Journal of Earthquake Engineering, 10, 207–236.

Friedl, M. A., Sulla-Menashe, D., Tan, B., Schneider, A., Ramankutty, N., Sibley, A., and Huang, X. (2010). MODIS Collection 5 global land cover: Algorithm refinements and characterization of new datasets. Remote Sensing of Environment, 114, 168–182.

Geiß, C., Taubenböck, H. (2012) Remote sensing contributing to assess earthquake risk: from a literature review towards a roadmap. Natural Hazards, 1-42. doi: 10.1007/s11069-012-0322-2.

GEM (2011) Global earthquake model. Available at http://www.globalquakemodel.org/. [Accessed 4 Dec 2013].

Joint Research Center (JRC) (2012) A Global Human Settlement Layer from Optical High Reolution Imagery. JRC Scientific and Policy Report EUR 25662 EN.

Joint Research Centre (2003) Global Land Cover 2000 database. Available at: http://bioval.jrc.ec.europa.eu/products/glc2000/glc2000.php Accessed 27 Sept 2013.

Langford, M., Higgs, G., Radcliffe, J., White, S. (2008) Urban population distribution models and service accessibility estimation. Computers, Environment and Urban Systems, 32, 66-80.

Mayaux, P., Hugh, E., Gallego, J., Strahle, A.H., Herold, M., Agrawal, S., Naumov, S., De Miranda, E.E., Di Bella, C.M., Ordoyne, C., Kopin, Y., Roy, P.S. (2006) Validation of the Global Land Cover 2000 Map. IEEE Transactions on Geoscience and Remote Sensing, 44, 1728-1739.

McPherson, J.M., Jetz, W., and Roegers, D.J. (2004) The effects of species' range sizes on the accuracy of distribution models: Ecological phenomenon or statistical fact? Journal of Applied Ecology, 41, 811-823.

Mennis, J., Hultgren, T. (2006) Intelligent daysmetric mapping and its application to aeal interpolation. Cartography and Geographic Information Science, 33, 179-194.

Mueller, M., Segl, K., Heiden, U., Kaufmann, H. (2006) Potential of high-resolution satellite data in the context of vulnerability of buildings. Natural Hazards, 38, 247–258.

Oak Ridge National Laboratory (ORNL) (2013) LandScan™ Available at: http://web.ornl.gov/sci/landscan/index.shtml [Accessed 4 Dec 2013]

Pesaresi, M., Guo, H., Blaes, X., Ehrlich, D., Ferri, S., Gueguen, L., Kalkia, M., Kauffmann, M., Kemper, T., Lu, L., Marin-Herrera., M.A., Ouzounis, G.K., Scavazzon, M., Soille, P., Syrris, V., Zanchetta, L. (2013) A Global Human Settlement Layer from optical HR/VHR RS data: concept and first results. IEEE Journal Of Selected Topics In Applied Earth Observations And Remote Sensing, 6, 2102-2131.

Pittore, M., Wieland, M. (2019) Towards a rapid probabilistic seismic vulnerability assessment using satellite and ground-based remote sensing. Natural Hazards, doi: 10.1007/s11069-012-0475-z, 2012.

Polli, D., Dell'Acqua, F. (2011) Fusion of optical and SAR data for seismic vulnerability mapping of buildings. In: Prasad, S., Bruce, L.M., Chanussot, J. (eds) Optical remote sensing. Advances in signal processing and exploitation techniques. Springer, Heidelberg, 329–341.

Potere, D., Schneider, A. (2009) Comparison of global urban maps, In: Global mapping of Human Settlement, In: Gamba, P. and M. Herold (Eds.), Global Mapping of Human Settlements: Experiences, Data Sets, and Prospects, Taylor and Francis, Boca Raton, FL.

Potere, D., Schneider, A., Angel, S., Civco, D.L. (2009) Mapping urban areas on a global scale: which of the eight maps now available is more accurate? International Journal of Remote Sensing, 30, 6531-6558.

RiskScape (2012) Easy-to-use multi-hazard impact and risk assessment tool. Available at http://www.globalquakemodel.org/. [Accessed 21 Nov 2013].

Sahar, L., Muthukumar, S., French, P. (2010) Using aerial imagery and GIS in automated building footprint extraction and shape recognition for earthquake risk assessment of urban inventories. IEEE Transactions in Geoscience and Remote Sensing, 48, 3511–3520.

Schneider, A., Friedl, M.A., Potere, D. (2009) A new map of global urban extent from MODIS data. Environmental Research Letters, 4, article 044003.

Schneider, A., Friedl, M.A., Potere, D. (2010) Monitoring urban areas globally using MODIS 500m data: New methods and datasets based on urban ecoregions. Remote Sensing of Environment, vol. 114, p. 1733-1746.

Socioeconomic Data and Applications Center (SEDAC) (2013): Global Rural-Urban Mapping Project (GRUMP), v1. Available at: http://sedac.ciesin.columbia.edu/data/collection/grump-v1 [Accessed 4 Oct 2013]

Taubenböck, H., Esch, T., Felbier, A., Roth, A., Dech, S. (2011) Pattern-based accuracy assessment of an urban footprint classification using TerraSAR-X data. IEEE Geoscience and Remote Sensing Letters, 8, 278-282.

Taubenböck, H., Esch, T., Felbier, A., Wiesner, M., Roth, A., and Dech, S. (2012) Monitoring urbanization in mega cities from space. Remote Sensing of the Environment, 117, 162-176.

Taubenböck, H., Post, J., Roth, A., Zosseder, K., Strunz, G., Dech, S. (2008) A conceptual vulnerability and risk framework as outline to identify capabilities of remote sensing. Natural Hazards and Earth System Sciences, 8, 409–420.

Taubenböck, H., Wurm, M., Setiadi, N., Gebert, N., Roth, A., Strunz, G., Birkmann, J., Dech, S. (2009) Integrating remote sensing and social science. Urban Remote Sensing Event, 2009, 1-7, doi: 10.1109/URS.2009.5137506.

United States Geological Survey (USGS) (2013) Land Cover Type Yearly L3 Global 500 m SIN Grid – MCD12Q1. Available at: https://lpdaac.usgs.gov/products/modis_products_table/mcd12q1 [Accessed 15 Dec 2013].

Wieland, M., Pittore, M., Parolai, S., Zschau, J., Moldobekov, B., Begaliev, U. (2012) Estimating building inventory for rapid seismic vulnerability assessment: towards an integrated approach based on multisource imaging. Soil Dynamics and Earthquake Engineering, 36, 70–83.